A novel application of the *S*-transform in removing powerline interference from biomedical signals

2009 Physiol. Meas. 30 13

(http://iopscience.iop.org/0967-3334/30/1/002)

IOP PUBLISHING PHYSIOLOGICAL MEASUREMENT

Physiol. Meas. **30** (2009) 13–27 doi:10.1088/0967-3334/30/1/002

A novel application of the *S*-transform in removing powerline interference from biomedical signals

Chien-Chun Huang[1], **Sheng-Fu Liang**[2], **Ming-Shing Young**[1] **and Fu-Zen Shaw**[3,4,5]

[1] Department of Electrical Engineering, National Cheng Kung University, Tainan 701, Taiwan
[2] Department of Computer Science and Information Engineering, National Cheng Kung University, Tainan 701, Taiwan
[3] Institute of Cognitive Science, National Cheng Kung University, Tainan 701, Taiwan
[4] Department of Physical Therapy, National Cheng Kung University, Tainan 701, Taiwan
[5] Biomimatic Systems Research Center, National Chiao Tung University, Hsinchu 300, Taiwan

E-mail: fzshaw@yahoo.com.tw

Received 28 May 2008, accepted for publication 13 October 2008
Published 27 November 2008
Online at stacks.iop.org/PM/30/13

Abstract

Powerline interference always disturbs recordings of biomedical signals. Numerous methods have been developed to reduce powerline interference. However, most of these techniques not only reduce the interference but also attenuate the 60 Hz power of the biomedical signals themselves. In the present study, we applied the *S*-transform, which provides an absolute phase of each frequency in a multi-resolution time–frequency analysis, to reduce 60 Hz interference. According to results from an electrocardiogram (ECG) to which a simulated 60 Hz noise was added, the *S*-transform de-noising process restored a power spectrum identical to that of the original ECG coincident with a significant reduction in the 60 Hz interference. Moreover, the S-transform de-noised the signal in an intensity-independent manner when reducing the 60 Hz interference. In both a real ECG signal from the MIT database and natural brain activity contaminated with 60 Hz interference, the *S*-transform also displayed superior merit to a notch filter in the aspect of reducing noise and preserving the signal. Based on these data, a novel application of the *S*-transform for removing powerline interference is established.

Keywords: powerline interference, *S*-transform, notch filter, ECG, EEG

1. Introduction

Powerline interference is an annoying problem which exists in many electrophysiological recordings (Huhta and Webster 1973), and it can strongly distort biopotentials. Numerous

biomedical signals, such as electrocardiogram (ECG) and electroencephalogram (EEG), contain distinct features in the time-domain analysis. For example, R-peak detection of an ECG is the first step in analyzing heart rate variability to assess autonomic nervous activity (Task Force of the European Society of Cardiology and the North Society of Pacing and Electrophysiology 1996). If an ECG is contaminated by powerline noise, the R-peak timing cannot be accurately measured. Afterward, functional assessment of the autonomic nervous system by means of heart rate variability is not convincing. Therefore, the noise needs to be minimized to extract critical features of the biopotentials. Several hardware-based techniques (Huhta and Webster 1973, Ott 1976, Thakor and Webster 1980, Shaw *et al* 2003), including twitching recording wires and shielding wires, have been used to reduce the influence of power interference. In almost all hardware systems, powerline noise is eliminated by either a low-pass or notch filter with a proper cutoff frequency. In fact, most bioelectric activities contain considerable power near or at the powerline frequency. Thus, a notch filter always attenuates the magnitude of both the biopotential and the noise around the powerline frequency. We set out to develop an optimal filter of preserving biopotentials while significantly reducing the powerline interference.

In addition to hardware treatment, several software techniques (Barr and Chan 1986, Pottala *et al* 1990, Ferdjallah and Barr 1994), including adaptive filters and independent component analysis for multichannel recordings, have been used to minimize powerline contamination. These methods require multiple channel inputs, including a reference recording of the interference from ac power. In the present study, we considered an alternative method to remove the energy of powerline interference without attenuating the biosignals from a single-channel recording. In general, system power is stationary throughout the recording session under a quiescent resting condition. Thus, the phase of the powerline interference should be constant. A more recent time–frequency representation, the *S*-transform (Stockwell *et al* 1996), has been demonstrated to provide multi-resolution analysis while retaining the absolute phase of each frequency. Therefore, the *S*-transform precisely extracts the phase of valuable signals in many fields, such as geophysics (Pinnegar and Mansinha 2003), medicine (Assous *et al* 2005) and power quality analysis (Dash *et al* 2003). In the present study, we employed the *S*-transform to decompose, estimate and extract the noise component arising from powerline interference to de-noise a signal. Characteristics of the time and frequency domains were compared between simulated and realistic biopotentials after a notch filter and the *S*-transform de-noising process.

2. Materials and methods

2.1. S-transform

The *S*-transform is an extension of the continuous wavelet transform (CWT) and is based on a moving and scalable localized Gaussian window. The *S*-transform is computed by shifting the window function down the signal in time across a range of frequencies. It is defined as

$$S_x(f,\tau) = \int_{-\infty}^{\infty} x(t)g(f,\tau,-t)\,\mathrm{e}^{-\mathrm{j}2\pi f t}\,\mathrm{d}t, \tag{1}$$

where $g(f, t)$ is a normalized Gaussian window. The width of the Gaussian window is determined by the examined frequency. The equation is given by

$$g(f,t) = \frac{1}{\sigma(f)\sqrt{2\pi}}\,\mathrm{e}^{-(t^2/2\sigma^2(f))}, \tag{2}$$

where $\sigma(f)$ is used to decide the width of the window. Similar to a wavelet, the value of $\sigma(f)$ is inversely proportional to the frequency f and can be denoted as

$$\sigma(f) = \frac{1}{a + b|f|}. \tag{3}$$

An inverse relationship between the frequency and window width is used. In other words, the window is narrower at higher frequencies and wider at lower frequencies. In equation (3), if $b = 0$, $\sigma(f)$ is a constant value that results in a constant window width. Therefore, the time–frequency analysis is similar to a short time Fourier transformation (STFT); if $a = 0$, the value of $\sigma(f)$ decreases as the frequency increases. It forms an *S*-transform. By substitution of equations (2) and (3) into (1), the equation of the *S*-transform can be more clearly stated as

$$S_x(f, \tau) = \int_{-\infty}^{\infty} x(t) \frac{b|f|}{\sqrt{2\pi}} \mathrm{e}^{\frac{-(\tau - t)^2 f^2 b^2}{2}} \mathrm{e}^{-\mathrm{j}2\pi f t}\, \mathrm{d}t, \qquad f \neq 0. \tag{4}$$

The *S*-transform can also be obtained by multiplying the CWT with the phase correction factor:

$$S_x(f, \tau) = \mathrm{e}^{-\mathrm{j}2\pi f \tau} W(f, \tau), \tag{5}$$

where $W(f, \tau)$ is the CWT. The phase of the *S*-transform referenced to the time origin provides useful and supplementary information about the spectra that is not available from locally referenced phase information in the CWT. Therefore, the *S*-transform contains the advantages of both STFT and CWT. Additionally, the *S*-transform can be implemented using fast Fourier transformation (FFT), and it also preserves the advantage of computation efficiency. Figure 1 shows the time–frequency chart of a 60 Hz sinusoid waveform using the *S*-transform. The peak amplitude is located at 60 Hz, and the absolute phase of 60 Hz is $-\pi/2$ throughout the entire window.

The *S*-transform is a linear operation on a signal $m(t)$. If noise $\eta(t)$ is added to the signal $m(t)$, it can be modeled as $m_{\text{noise}}(t) = m(t) + \eta(t)$. The *S*-transform gives

$$S\{m_{\text{noise}}(t)\} = S\{m(t)\} + S\{\eta(t)\}. \tag{6}$$

The linear property of the *S*-transform is greatly beneficial for the de-noising process through the subtraction of the powerline interference.

2.2. Implementation of the S-transform

$X(f)$ is the Fourier spectrum of $x(t)$. The *S*-transform in the frequency domain is given by

$$S_x(f, \tau) = \int_{-\infty}^{\infty} X(\alpha + f)\, \mathrm{e}^{-2(\pi\alpha/bf)^2} \mathrm{e}^{\mathrm{j}2\pi\alpha\tau}\, \mathrm{d}\alpha, \qquad f \neq 0. \tag{7}$$

Using discrete Fourier transformation (DFT) and inverse DFT (IDFT), the discrete *S*-transform of time series $x[n]$ is represented as

$$\begin{aligned} S_x[k, \ell] &= \frac{1}{N} \sum_{m=0}^{N-1} X[m + k] G[k, m]\, \mathrm{e}^{\frac{\mathrm{j}2\pi m\ell}{N}}, \qquad k \neq 0 \qquad \text{and} \\ S_x[0, \ell] &= \frac{1}{N} \sum_{n=0}^{N-1} x[n] = \frac{1}{N} X[0], \qquad k = 0, \end{aligned} \tag{8}$$

where $\ell, m, k = 0, 1, 2, \ldots, N - 1$, N is the total number of sampling points and $G[k, m]$ is derived from the DFT of the Gaussian window $g(f, t)$. The equations defining $G[k, m]$ are

$$G[k, m] = \begin{cases} \mathrm{e}^{-2(\pi m/bk)^2}, & \text{if} \quad 0 \leqslant m \leqslant (N/2 - 1) \\ \mathrm{e}^{-2(\pi(m-N)/bk)^2}, & \text{if} \quad (N/2) \leqslant m \leqslant (N - 1). \end{cases} \tag{9}$$

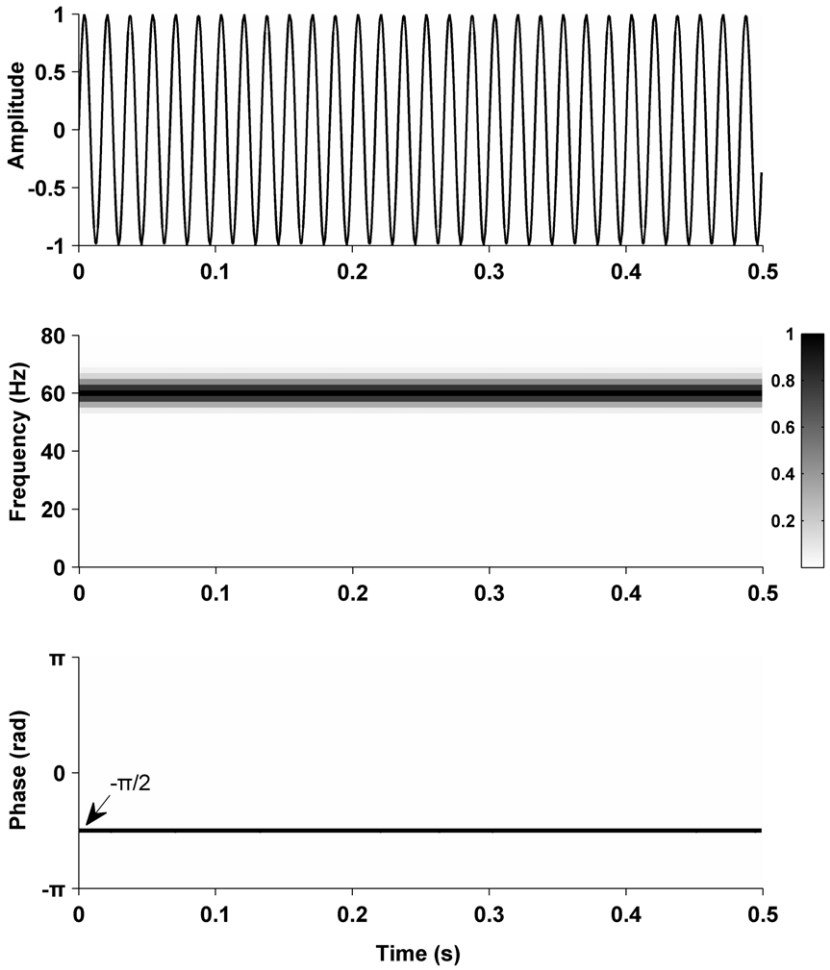

Figure 1. *S*-transform of a 60 Hz sine waveform. Panels from top to bottom display an original 60 Hz sine wave, and its amplitude and phase in a time–frequency presentation. A constant phase, $-\pi/2$, is shown in the phase spectrum.

The implantation flowchart of the discrete *S*-transform is sketched in figure 2. The discrete version of the *S*-transform (equation (8)) was calculated by the FFT, and the computational complexity of the *N*-point FFT is $N \log N$. Data series and Gaussian window were transferred into a frequency domain using the *N*-point FFT. To reduce the computation time, only each time shift point m at target frequency k_p (60 Hz herein) was calculated. Thus, $X[m + k_p]$ should be element-by-element multiplied by the Gaussian window $G[k_p, m]$ which needs N additional operations. Therefore, the computational complexity of the *S*-transform here may be $N + 2N \log N$ (in terms of the number of arithmetic operations required).

2.3. Software

The algorithm of the *S*-transform was implemented with Matlab and embedded into a LabVIEW platform (National Instruments, Austin, TX). The power spectra of simulated and

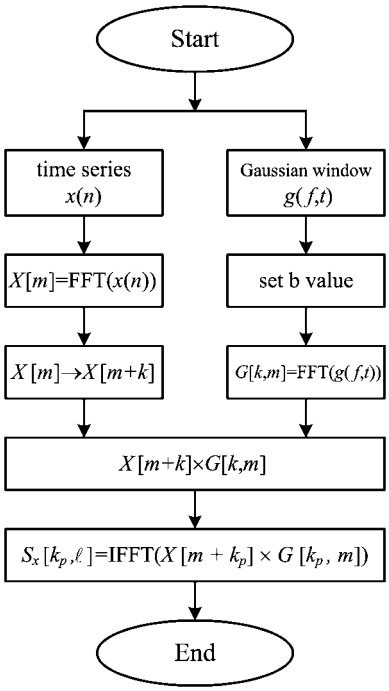

Figure 2. Flowchart of a discrete *S*-transform.

realistic signals were calculated by the FFT with a Hanning window that attenuated spectral leakage due to edge discontinuities. The notch filter adopted in the study was a second-order digital IIR filter implemented by Digital Filter Design Toolkit (National Instruments, Austin, TX). The transfer function of a second-order notch filter is expressed as

$$T(s) = a_2 \frac{s^2 + \omega_o^2}{s^2 + (\omega_o/Q)s + \omega_o^2},$$

where ω_o and Q are the notch frequency and quality factor, respectively. The Q value reflects a sharpness of the stop bandwidth of the filter. In general, increasing the Q factor results in narrowing the stop bandwidth and less power attenuation of the notch frequency. A bilinear transform can convert the s-domain transfer function into a discrete z-domain function for digital notch filters.

2.4. Subjects and data acquisition

2.4.1. Human ECG recording. A two-lead ECG with lead II configuration was recorded from a healthy subject's chest with Ag/AgCl electrodes by using a battery-powered ECG recorder (digitized at 500 Hz with a gain of 1000 at 0.1–100 Hz). The ECG was used as a basis because of no obvious powerline interference. The QRS complex of the ECG contains wide spectral information, which displays great overlap with the frequency of the powerline interference. All simulation results shown below were primarily based on extracting accurate R-peak information. In addition, a dataset (103.dat) from the MIT-BIH Arrhythmia Database (http://www.physionet.org) was used to evaluate de-noising effectiveness for realistic ECG contaminated with 60 Hz noise.

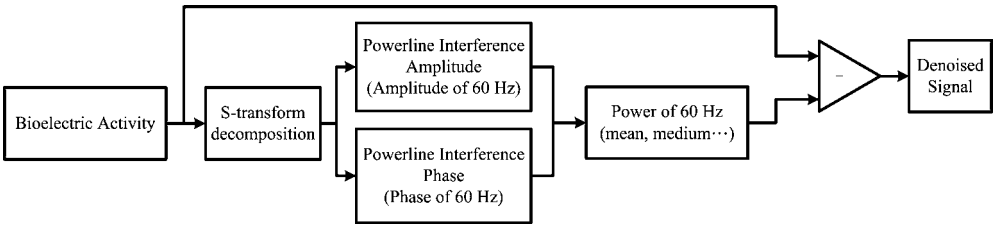

Figure 3. Diagram of the de-noising procedures using the *S*-transform.

2.4.2. Rat EEG recording. Cortical field potentials of a Long-Evans rat with remarkable 60 Hz interference were recorded. All surgical and experimental procedures performed in rats were reviewed and approved by the Institutional Animal Care and Use Committee of National Cheng Kung University. The animal preparation, the signal conditioning circuit and the data acquisition system were described elsewhere in detail (Shaw *et al* 1999, 2002). In brief, skull screw electrodes were bilaterally implanted in the areas of the frontal, parietal and occipital cortices in anesthetized Long-Evans rats. A ground electrode was fixed onto the skull over the cerebellum. After 3 weeks recovery, cortical field potentials were recorded from chronically implanted skull electrodes in freely moving rats. A buffer headset (with a gain of 1) was connected to the rat's head to conduct the EEG into the post-amplifier system with a gain of 5000 in the range of 0.3–70 Hz. Spontaneous spike-wave discharges (SWDs), which are associated with absence seizures (Shaw 2004, 2007), are often observed in Long-Evans rats. In the present study, a noisy EEG reading was obtained without careful grounding in the freely moving rat.

2.5. De-noising process

The de-noising procedure is illustrated in figure 3. Bioelectrical activity contaminated with powerline interference was first decomposed by the *S*-transform to extract the amplitude and phase array. Afterward, the possible amplitude and phase of the powerline interference were estimated with regard to several reference derivations (see details in the following section). The power of the possible interference, which was derived from the estimated amplitude and phase, was calculated and then subtracted from the original signal. Therefore, the de-noising process for bioelectrical activity was completed. In the de-noising procedure using the *S*-transform, two aspects of parameters had to be determined: methods for the estimation of amplitude and phase and the time–frequency window parameter b.

3. Choosing optimal parameters of the *S*-transform

Under a resting condition which is used in most cases in practice, the powerline interference appearing in the recording exhibited no large fluctuations. Based on this important phenomenon, the amplitude and phase of the interference may be constant within a short period, i.e. a few seconds. On the other hand, most biomedical signals cover a wide frequency range, which overlaps with the powerline frequency. For instance, the QRS complex of the ECG contains a 60 Hz amplitude. Thus, the 60 Hz amplitude of most bioelectrical activities changes with time, and it would not be a constant value within a small time–frequency window. When both the biopotential and powerline interference were mixed under a realistic condition, a fluctuating amplitude and phase were observed at 60 Hz. According to the properties of both a constant interference and random fluctuations of the biosignal, a de-noising process using the

Table 1. Comparison of 60 Hz powers after *S*-transform with regard to various references (median, mean, minimum and maximum) under two proportional data populations (75% and 100%). Test signals ($n = 10$) were an electrocardiogram (-69.30 ± 0.18 dB at 60 Hz) to which was added 60 Hz sinusoidal noise (0.5 mV, $-\pi/2$).

	75% of the amplitude			100% of the amplitude		
Method	Amplitude (mV)	Phase (radian)	Power (dB)	Amplitude (mV)	Phase (radian)	Power (dB)
Median	0.500 ± 0.000	-1.571 ± 0.002	-64.75 ± 4.48[a]	0.500 ± 0.000	-1.571 ± 0.002	-64.75 ± 4.48[a]
Mean	0.500 ± 0.000	-1.571 ± 0.000	-69.38 ± 0.27	0.501 ± 0.001	-1.571 ± 0.000	-67.39 ± 2.79[a]
Minimum	0.496 ± 0.001	-1.687 ± 0.040	-28.24 ± 3.12[a]	0.448 ± 0.019	-1.687 ± 0.040	-25.52 ± 2.29[a]
Maximum	0.504 ± 0.001	-1.432 ± 0.036	-26.45 ± 2.91[a]	0.561 ± 0.018	-1.432 ± 0.036	-23.31 ± 1.46[a]

Data are presented as the mean $\pm$ standard deviation.
[a] $p < 0.05$ versus the original 60 Hz power electrocardiogram by the paired *t*-test.

S-transform was constructed to filter out the powerline interference through a single-channel biopotential.

3.1. Four derivations for estimating the amplitude and phase of the powerline interference

An artificial 60 Hz sinusoidal wave of 0.5 mV amplitude was added to a raw ECG (-69.30 ± 0.18 dB at 60 Hz). Four references, i.e. the mean, median, minimum and maximum, were compared to estimate the amplitude and phase which contributed to the 60 Hz powerline interference. Additionally, two populations of samples (75% and 100% in table 1) were used to calculate the reference. The QRS complex possessing considerable power at 60 Hz can lead to large fluctuations in particular time windows. In a sorted amplitude or phase array after the *S*-transform, the distribution of the amplitude or phase samples always revealed a central peak accompanied by considerable probability in the two extremities of the sample population. To minimize the possible contribution of these two extremities, a 75% amplitude array was used to estimate the powerline noise level. In this case, the amplitude array was first sorted, and both the upper and lower 12.5% of the amplitude array were ruled out.

Table 1 displays a comparison of 60 Hz powers in four different methods under two sample populations ($n = 10$). The time–frequency window b was 1 (see the results in the following subsection). The amplitude and phase of the data population with regard to the mean or median derivations approximated the amplitude (0.5 mV) and phase ($-\pi/2$) of an artificial sinusoidal wave. After the *S*-transform de-noising process, almost all estimated 60 Hz powers revealed significant differences compared to the 60 Hz power of the original ECG (-69.30 ± 0.18 dB). Only the 60 Hz power estimated by the mean reference of the 75% data array (-69.38 ± 0.27 dB) showed no remarkable difference from that of the original ECG ($p = 0.295$). Most specifically, the amplitude and phase estimated using the *S*-transform with regard to the mean of the 75% data population were almost identical to those of the artificial sine wave. This might be the reason why the *S*-transform de-noising process performed well in the mean reference.

3.2. Effect of the time–frequency window parameter b in the de-noising process

The b value of the *S*-transform determines the window width for a given frequency (Stockwell *et al* 1996). In a previous study (Chilukuri and Dash 2004), the b value was suggested to be 0.333–5. To further determine the b factor in the *S*-transform de-noising process, differences between the estimated and realistic aspects of the amplitude and phase were compared

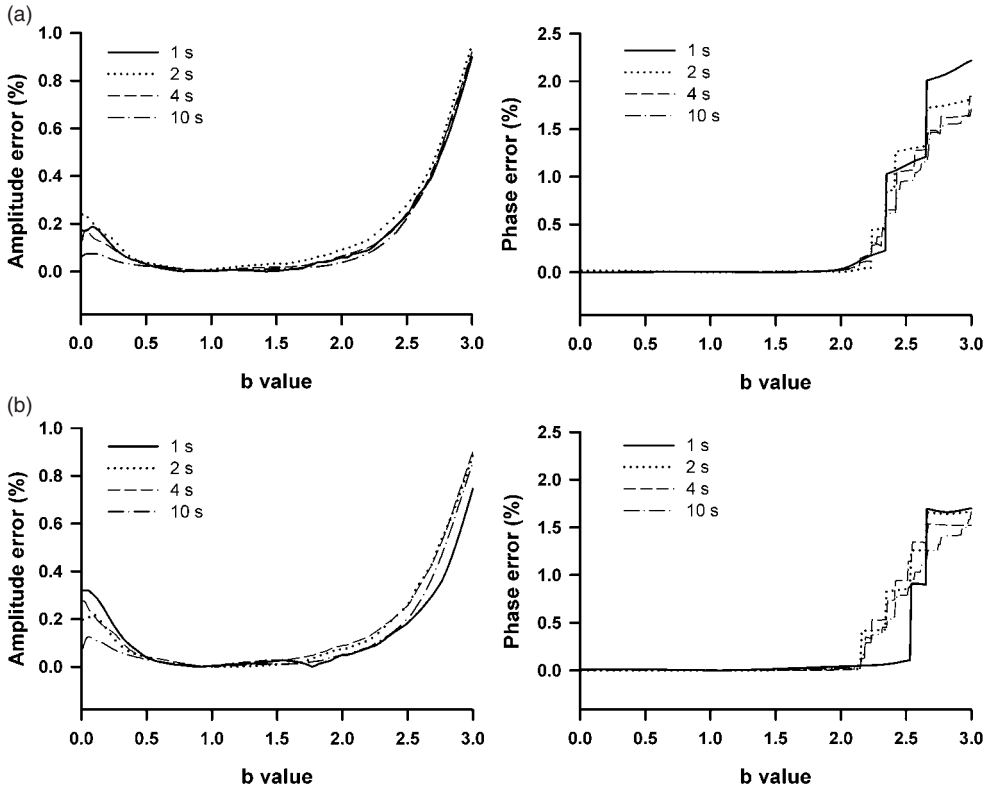

Figure 4. Effect of the time–frequency window b on errors of the 60 Hz amplitude and phase using the S-transform de-noising process with four different data lengths under two different sampling frequencies (250 Hz in (a) and 500 Hz in (b)). The test signals were original electrocardiograms with 0.5 mV sinusoidal noise. Errors of the amplitude and phase were defined as differences between the estimated and test data.

(figure 4). Under four different data lengths at two sampling frequencies (250 and 500 Hz), similar curves were found in the errors of the amplitude and phase with the b factor. The errors of amplitude and phase were minimal when the b value was in the range of 0.5–2. Furthermore, errors of the amplitude and phase occurring at $b = 1$ were consistently the lowest (figure 4). Outside this range, the amplitude showed dramatic increases at the two extremities. The phase error obviously increased when the b factor was larger than 2. Based on these results (table 1, figure 4), several criteria were determined in the following de-noising process of the S-transform: (1) $b = 1$, (2) the mean amplitude of the 75% population and (3) the mean phase of the 75% population.

4. De-noising performance using the *S*-transform

In the present study, the de-noising effects of both the notch filter and S-transform were compared. Figure 5 illustrates the temporal and frequency responses of the original ECGs adding an artificial 60 Hz sine wave and the filtered results (notch filter and S-transform). An obvious 60 Hz peak is shown in the power spectrum (figure 5(a)). Figure 5(b) depicts a clear ECG signal after the application of the S-transform de-noising process. In addition, the power

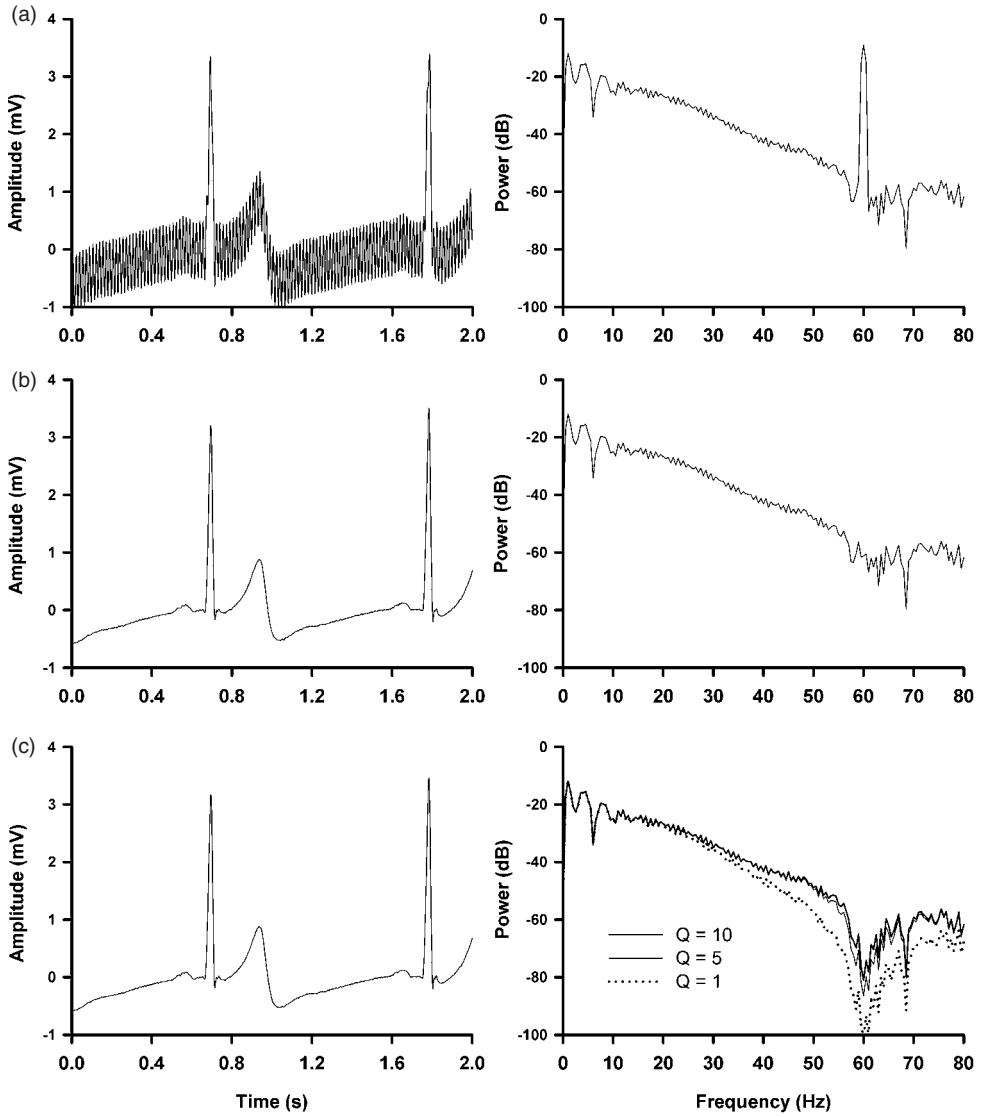

Figure 5. Representative examples of temporal electrocardiogram (ECG) traces (left) and their spectra (right) under different filter processes. (a) An ECG signal + artificial powerline interference (0.5 mV, 60 Hz) and its power spectrum, (b) an ECG trace after the *S*-transform de-noising and its power spectrum, (c) an ECG treated with a 60 Hz notch filter ($Q = 10$) and three power spectra of ECGs with notch filters ($Q = 1, 5, 10$).

spectrum after *S*-transform de-noising, except at 60 Hz, was identical to the original one. In sharp contrast, a large, wide trough was seen in the power spectrum using the notch filter ($Q = 10$) since a clear ECG was restored in the time domain (figure 5(c)). A notch filter of $Q = 1$ showed a wider trough and a larger power attenuation around 60 Hz compared to the other two Q values ($Q = 5$, 10). In order to quantify differences between these methods, the R-peak amplitude was measured ($n = 10$). A significant difference existed among all processes (figure 6; $p < 0.001$ by one-way repeated measures ANOVA on rank). The R-peak amplitude

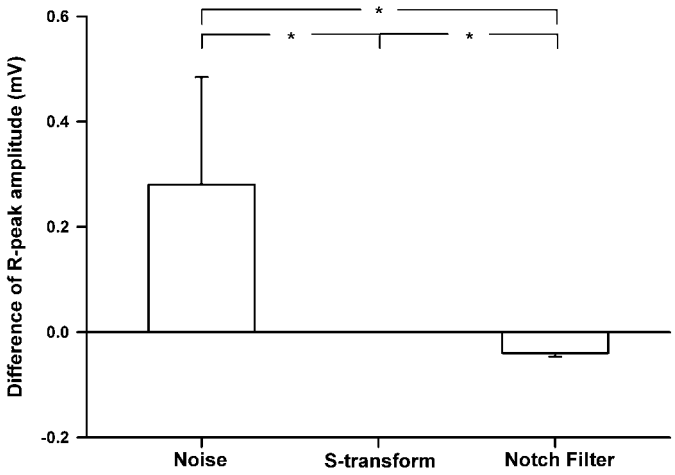

Figure 6. R-peak amplitudes with different processes compared to those of raw ECGs ($n = 10$). Three conditions were compared: **noise**, difference between the R-peak amplitude of a raw ECG and that of the raw ECG with an artificial 0.5 mV sine wave; **S-transform**, difference between the R-peak amplitude of a raw ECG and that after application of the *S*-transform de-noising process; and **notch filter**, difference between the R-peak amplitude of a raw ECG and that after application of a notch filter. Data are presented as the mean ± standard deviation. $^*p < 0.05$ by the Student–Newman–Keuls test.

subjected to the *S*-transform de-noising process revealed almost no difference compared to the original R-peak amplitude (0.000 ± 0.001 mV). However, the R-peak amplitude was significantly attenuated by the notch filter (−0.040 ± 0.007 mV).

Other than a constant 60 Hz amplitude, the performances of the notch filter with four different Q values and the *S*-transform at various levels of noise amplitude were also evaluated (figure 7). The 60 Hz power after the *S*-transform de-noising process revealed a constant value that was closely approximate to the 60 Hz power of original ECGs. Thus, the *S*-transform de-noising process seemed to be a noise level-independent process. On the other hand, the notch filter did not perform very well in reducing the 60 Hz interference. With a high-Q notch filter, 60 Hz power did not attain the level of the original ECG. In contrast, an over-reduction of 60 Hz power was seen under a low-Q condition (figure 7). Additionally, dramatic suppression of a wide frequency was also seen with the low-Q notch filter (figure 5(c)). The responsive curve of a notch filter of $Q = 10$ was approximate to the original ECGs. Thus, the notch filter of $Q = 10$ was used in assessment of realistic biomedical signals. Based on these simulated results, the *S*-transform de-noising process showed significant advantages for removing 60 Hz noise and preserving the power distribution of ECGs.

In addition, to compare the filter performance of simulated signals, realistic noisy biosignals were tested. As shown in figure 8, the *S*-transform de-noising process effectively eliminated the 60 Hz interference of the ECGs from the MIT-BIH Arrhythmia Database with no distortion in the powers of other frequencies. An over-attenuation was observed in the process of a notch filter. A normal EEG followed by a spontaneous SWD (marked by a bold line) is shown (figure 9(a)). From the temporal traces, more of the high-frequency component of the normal EEG activity was preserved by the *S*-transform de-noising process compared to that of the notch filter. Furthermore, the amplitude of the SWD using the *S*-transform de-noising process was also obviously higher than that of the notch filter. In addition, a clear and significant reduction of 60 Hz power (25 dB) without changing the powers of other

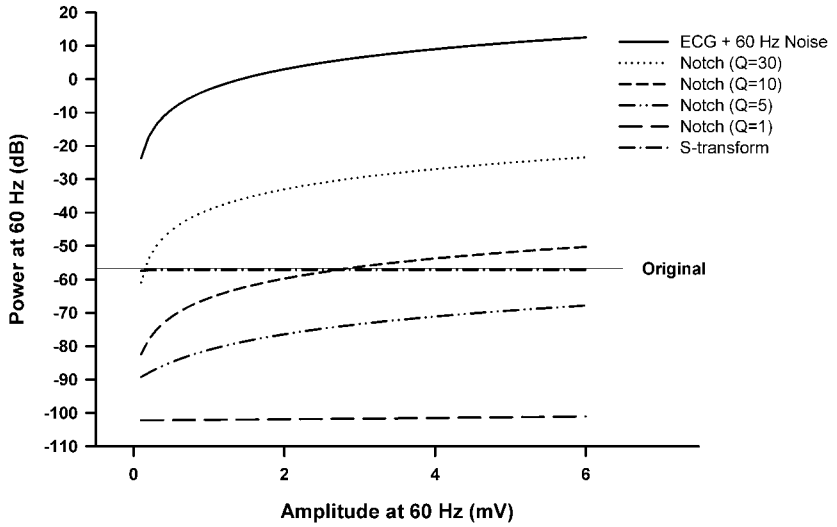

Figure 7. De-noising effects of the *S*-transform and notch filter with four different Q values under various 60 Hz amplitudes. The 60 Hz power after the *S*-transform de-noising process was independent of exogenous 60 Hz amplitudes. 60 Hz power of ECGs increased as Q value of a notch filter increased. Results of 60 Hz power with a $Q = 10$ notch filter are approximate to those of the original signal and *S*-transform.

frequency ranges was achieved after applying the *S*-transform de-noising process (figure 9(c)). In contrast, significant attenuation of powers at 60 Hz and its adjacent frequency range was illustrated by the notch filter (figure 9(d)). Although there is no answer about the accurate amplitude in realistic bioelectrical activity, the continuity in the power spectrum illustrates the advantage of our proposed *S*-transform de-noising process. Results from both the ECG and EEG signals indicated that the *S*-transform de-noising method is feasible and robust for removing powerline interference with no distortion of meaningful bioelectrical activity.

5. Discussion

In the present study, we provided evidence for the advantages of the de-noising performance of the *S*-transform based on results of both simulated and realistic signals. With *S*-transform de-noising, the power spectrum of the original bioelectrical activity was preserved, and 60 Hz powerline interference was significantly reduced. Results from the *S*-transform de-noising process were significantly better than those with a notch filter. Moreover, the *S*-transform de-noising process could be carried out in a single-channel recording without a reference signal, which is commonly used in adaptive filters (Ma *et al* 1999). In addition to previous applications of the *S*-transform (Dash *et al* 2003, Pinnegar and Mansinha 2003, Assous *et al* 2005), we created a new function for the *S*-transform which significantly reduced the powerline interference.

The *S*-transform produces a multi-resolution analysis with a constant relative bandwidth (Stockwell *et al* 1996, Chilukuri and Dash 2004). The b value of the *S*-transform determines the window width for a given frequency (Stockwell *et al* 1996). According to the Heisenberg uncertainty principle, a high precision in both time and frequency cannot simultaneously be obtained. A small b value forms a wide window width in high frequency ranges and vice versa for a high b value (Chilukuri and Dash 2004). In a previous study (Chilukuri and Dash 2004),

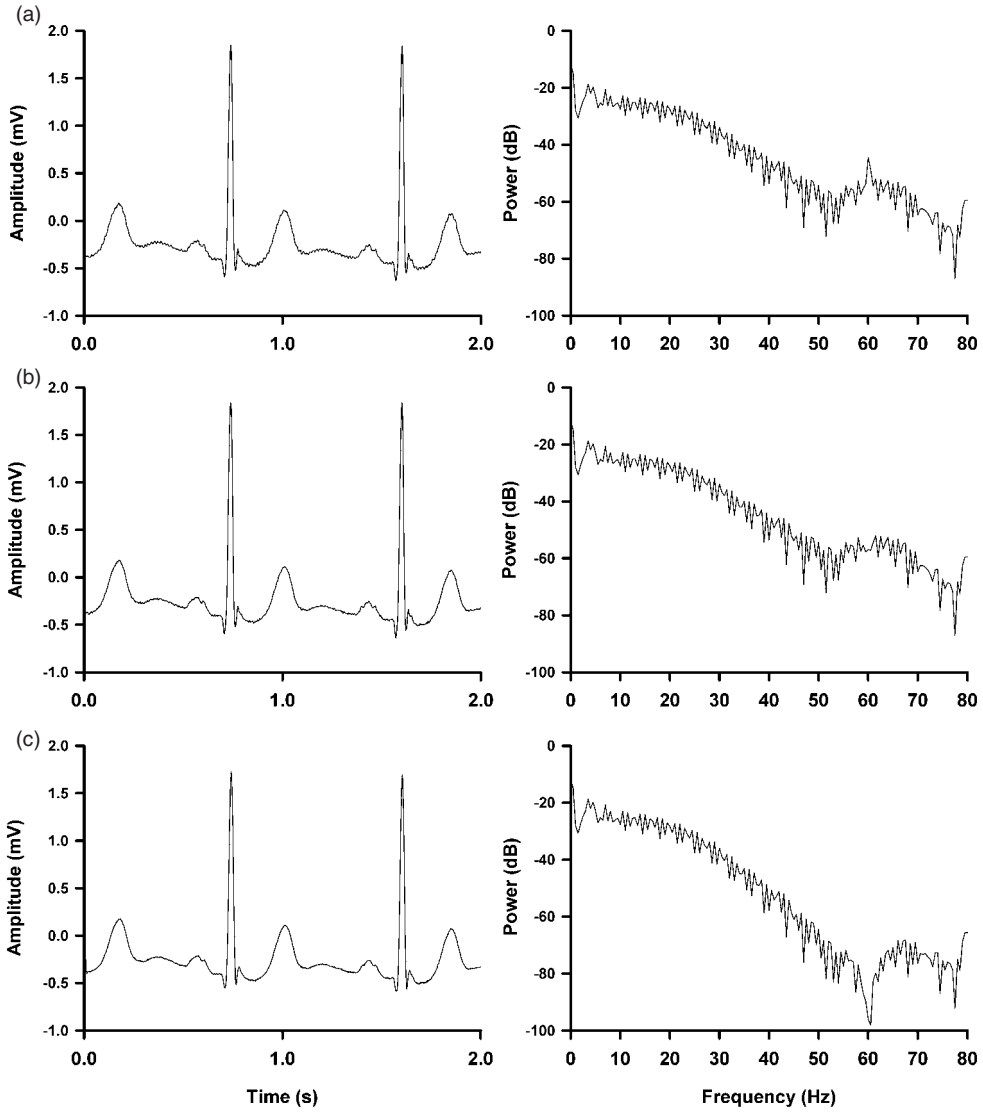

Figure 8. Representative examples of natural 60 Hz contaminated temporal ECG traces (left) and their spectra (right) from the MIT-BIH Arrhythmia Database. (a) A 2 s (sampling rate 360 Hz) ECG signal and its power spectrum, (b) an ECG trace after the *S*-transform de-noising and its power spectrum and (c) an ECG signal after application of a 60 Hz notch filter ($Q = 10$) and its power spectrum.

the b value was suggested to be 0.333–5 when applied to power delivery quality. In this study, a better range for b values was 0.5–2 as determined from errors of both amplitude and phase estimation (figure 4). A high b value (>2) was accompanied by a narrow window width, i.e. increasing the time resolution with poor frequency resolution. Poor frequency resolution may result in less power concentrated in the powerline interference, and may subsequently produce a great error in the powerline frequency. On the other hand, a small b value (<0.5) had a high frequency resolution accompanied by poor temporal resolution. In general, the powerline frequency slightly fluctuates around a particular frequency (60 Hz in the present

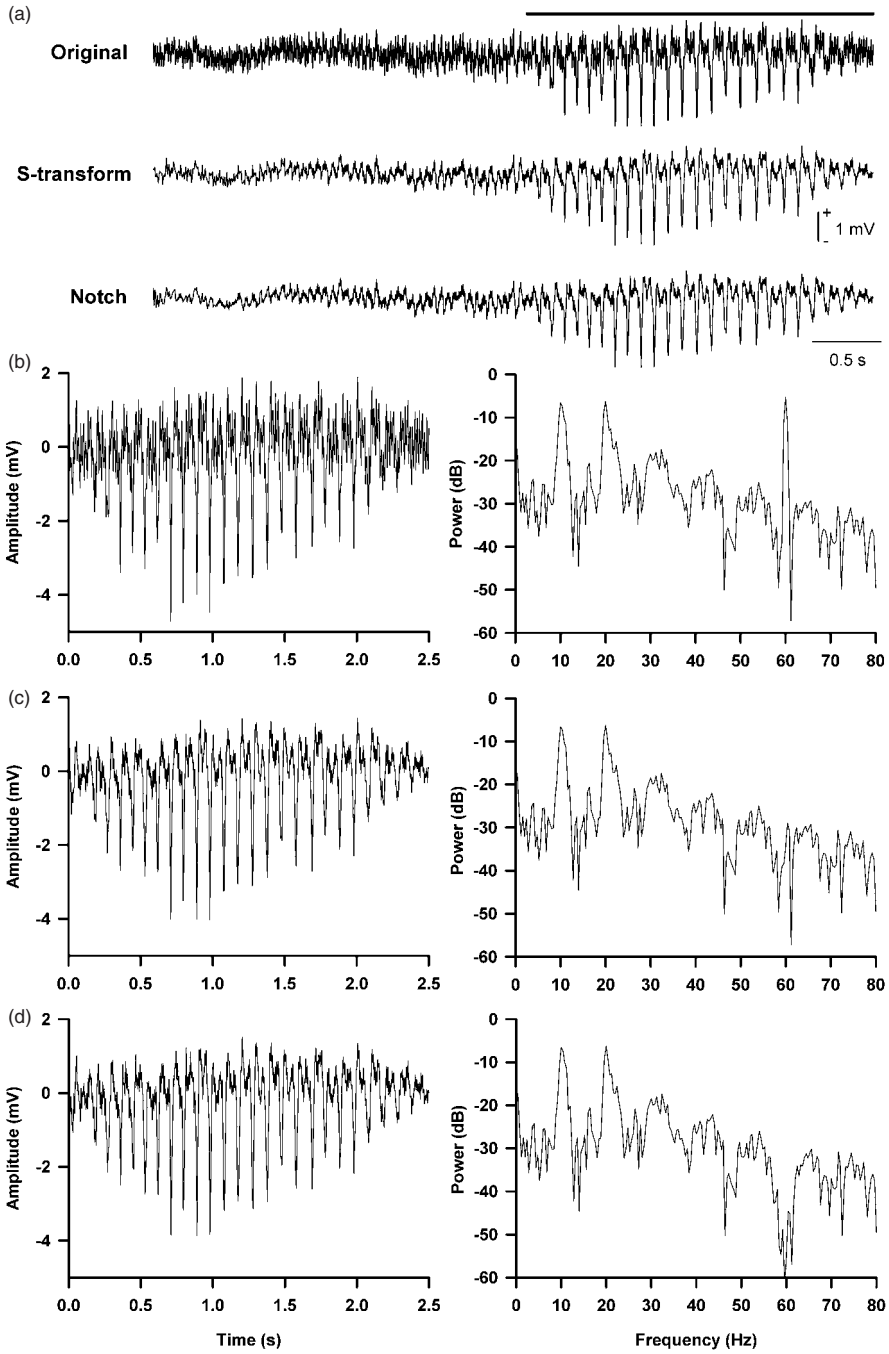

Figure 9. A representative example of brain activity and the de-noising results. (a) Temporal traces of the brain activity in a freely moving rat from top to bottom are the original noisy activity, the *S*-transform de-noising activity and activity after application of a notch filter. A spontaneous SWD appearing in a Long-Evans rat is marked by a bold line. (b) Temporal trace (left) and power spectrum (right) of the marked SWD. (c) Temporal trace and power spectrum of the marked SWD after applying the *S*-transform de-noising process. (d) Temporal trace and power spectrum of the marked SWD after applying a notch filter with $Q = 10$.

study). The resolution of the frequency domain that is too high might produce an uncertainty in the accuracy of the powerline frequency, and a great error may be obtained. Based on our simulation, errors of both the amplitude and phase were consistently low at $b = 1$, which was used in the entire study. Accordingly, a value of $b = 1$ is optimal for de-noising processes using the *S*-transform.

A stable and constant powerline frequency is assumed for the application of the *S*-transform de-noising process. In general, the delivery quality of a power, including its frequency, is well controlled. The powerline frequency during power delivery falls in the range of 60 $\pm$ 0.1 Hz with a very high probability (96.74%) in a half-year power monitoring of Taiwan Power Company. The fluctuation of the powerline frequency falling in the range of 0.11–0.3 Hz is 3.25%. Only 0.01% of the powerline frequency fluctuates >0.3 Hz. A tiny frequency fluctuation should not be observed in a short time window. For a 2 s data segment (0.5 Hz frequency resolution) used in this study, the major peak of powerline interference should basically be located at 60 Hz in most cases. In our examples of real ECG signals from the MIT-BIH Arrhythmia Database and natural brain activities from a rat, the 60 Hz power peak can be seen (figures 8(a) and 9(a)). The fluctuation of the powerline frequency in these real biosignals is very rare (1.55% of 30 min data segments ($n = 902$) in the MIT-BIH Database and 0% of 280 s data segment ($n = 140$) in rat EEGs). Thus, the powerline frequency is generally stationary. Several aspects of results obtained in this study also supported that the *S*-transform de-noising process worked very well in canceling out 60 Hz powerline interference and preserving the original signals.

According to our assumption of the *S*-transform de-noising process, our method would not filter out transient noise, such as transient power spikes. In that case, an adaptive filter with a power monitor may be a better alternative (Ferdjallah and Barr 1994, Ma *et al* 1999). On the other hand, powerline interference of biomedical signals may display a primary peak accompanied by several harmonics (Huhta and Webster 1973). Because frequency fluctuations of these harmonics are not generally large, an *S*-transform comb filter, which is based on our proposed de-noising process at a single frequency, should be established to reduce all contributions from the power line.

In much clinical or basic research, a long-term biosignal recording is required, such as intensive care unit ECGs. For a long data segment, the powerline frequency is not sure to be 60 Hz because of its increased frequency resolution. The *S*-transform de-noising process may not work well in long-duration data. However, our results have strongly supported the *S*-transform de-noising process working in eliminating the powerline interference and preserving the original signal spectrum with a 2 s data window. Accordingly, long-term bioelectric data could be cut into fixed and short length segments, for instance 2 s here. Following this, a subsequent *S*-transform de-noising process is carried out slide by slide. A good quality signal should be seen.

In many biomedical systems, a notch filter is a fixed selection to eliminate the powerline interference. However, the notch filter not only reduces the powerline interference but also attenuates the power around the powerline frequency. Moreover, the notch frequency of a notch filter often drifts with temperature, and elements of notch filters gradually degrade with time. These disadvantages have generated great concerns in applying notch filters to biomedical signals (Pottala *et al* 1990, Breithardt *et al* 1991). In the present study, we provided several lines of evidence on the advantages of the *S*-transform de-noising process in eliminating powerline interference in coincidence with maintaining the power of the original signals. Besides, the *S*-transform can be implanted using a standard DFT or FFT algorithm (Stockwell *et al* 1996, Chilukuri and Dash 2004). The DFT and FFT algorithms have been demonstrated to be capable of being implanted using a generic digital signal processor chip

(Lakshmikanth and Morcos 2001, Salem *et al* 2007). Accordingly, an *S*-transform chip might be a next step for real-time reduction of powerline interference.

Acknowledgments

We thank Mr Chien-Hung Huang for providing technical support in implementing the *S*-transform. This work was supported by the National Science Council (NSC97-2627-B-006-006 and NSC97-2220-E-006-009), Taiwan. The authors declare no conflict of interest.

References

Ahlstrom M L and Tompkins W J 1985 Digital filters for real-time ECG signal processing using microprocessors *IEEE Trans. Biomed. Eng.* **32** 708–13

Assous S, Humeau A, Tartas M, Abraham P and L'Huiller J P 2005 Physiological effects of indomethacin and celecobix: an S-transform laser Doppler flowmetry signal analysis *Phys. Med. Biol.* **50** 1951–9

Barr R E and Chan E K Y 1986 Design and implementation of digital filters for biomedical signal processing *J. Electrophysiol. Technol.* **13** 73–93

Breithardt G, Cain M E, el-Sherif N, Flowers N C, Hombach V, Janse M, Simson M B and Steinbeck G 1991 Standards for analysis of ventricular late potentials using high-resolution or signal-averaged electrocardiography. A statement by a Task Force Committee of the European Society of Cardiology, the American Heart Association, and the American College of Cardiology *Circulation* **83** 1481–8

Chilukuri M V and Dash P K 2004 Multiresolution S-transform-based fuzzy recognition system for power quality events *IEEE Trans. Power Deliv.* **19** 323–30

Dash P K, Panigrahi B K and Panda G 2003 Power quality analysis using S-transform *IEEE Trans. Power Deliv.* **18** 406–11

Ferdjallah M and Barr R E 1994 Adaptive digital notch filter design on the unit circle for the removal of powerline noise from biomedical signals *IEEE Trans. Biomed. Eng.* **41** 529–36

Huhta J C and Webster J G 1973 60-Hz interference in electrocardiography *IEEE Trans. Biomed. Eng.* **20** 91–101

Lakshmikanth A and Morcos M M 2001 A power quality monitoring system: a case study in DSP-based solutions for power electronics *IEEE Trans. Instrum. Meas.* **50** 724–31

Ma W K, Zhang Y T and Yang F S 1999 A fast recursive-least-squares adaptive notch filter and its applications to biomedical signals *Med. Biol. Eng. Comput.* **37** 99–103

Ott H W 1976 *Noise Reduction Techniques in Electronic Systems* (New York: Wiley) pp 54–90

Pinnegar C R and Mansinha L 2003 The S-transform with windows of arbitrary and varying shape *Geophysics* **68** 381–5

Pottala E W, Horton M R and Bailey J J 1990 Suppression of powerline interference in the ECG signal using a bilinearly transformed null phase notch filter *J. Electrocardiol.* **23** (Suppl) 213–4

Salem M E, Mohamed A and Samad S A 2007 Fast detection and classification of power quality disturbances based on DSP implementation *Int. Rev. Electr. Eng.* **2** 163–70

Shaw F Z 2004 Is spontaneous high-voltage rhythmic spike discharge in Long Evans rats an absence-like seizure activity? *J. Neurophysiol.* **91** 63–77

Shaw F Z 2007 7–12 Hz high-voltage rhythmic spike discharges in rats evaluated by antiepileptic drugs and flicker stimulation *J. Neurophysiol.* **97** 238–47

Shaw F Z, Chen R F, Tsao H W and Yen C T 1999 A multichannel system for recording and analysis of cortical field potentials in freely moving rats *J. Neurosci. Methods* **88** 33–43

Shaw F Z, Lai C J and Chiu T H 2002 A low-noise flexible integrated system for recording and analysis of multiple electrical signals during sleep-wake states in rats *J. Neurosci. Methods* **118** 77–87

Shaw F Z, Yen C T and Chen R F 2003 A simple and effective process for noise reduction of multichannel cortical field potential recordings in freely moving rats *J. Neurosci. Methods* **124** 167–74

Stockwell R G, Mansinha L and Lowe R P 1996 Localization of the complex spectrum: the S transform *IEEE Trans. Signal Process.* **44** 998–1001

Task Force of the European Society of Cardiology and the North Society of Pacing and Electrophysiology 1996 Heart rate variability: standards of measurement, physiological interpretation, and clinical use *Circulation* **93** 1043–65

Thakor N V and Webster J G 1980 Ground-free ECG recording with two electrodes *IEEE Trans. Biomed. Eng.* **27** 699–704